Frequency response and origin of the spin-1/2 photoluminescence-detected magnetic resonance in a π-conjugated polymer

M. Segal and M. A. Baldo*
Department of Electrical Engineering, Massachusetts Institute of Technology, Cambridge, Massachusetts 02139, USA

M. K. Lee and J. Shinar*
Ames Laboratory–USDOE and Department of Physics and Astronomy, Iowa State University, Ames, Iowa 50011-3160, USA

Z. G. Soos
Department of Chemistry, Princeton University, Princeton, New Jersey 08544, USA
(Received 6 October 2004; revised manuscript received 26 January 2005; published 15 June 2005)

We model the frequency responses of the photoinduced absorption (PA) and the spin-1/2 photoluminescence-detected magnetic resonance (PLDMR) in the archetypal π-conjugated polymer poly[2-methoxy-5-(2-ethylhexyloxy)-1,4-phenylenevinylene]. We show that the frequency response of the resonance is consistent with a quenching model mediated by spin-dependent interactions between triplet excitons and polarons. Two polaron populations are identified: short-lived paired polarons that may recombine after spin-dependent collisions with triplet excitons, and long-lived unpaired polarons that are unaffected by microwave resonance. The large density of unpaired polarons dominates the frequency response of PA measurements, but does not influence the frequency response of the PLDMR, which instead probes the dynamics of triplet excitons and paired polarons.

DOI: 10.1103/PhysRevB.71.245201 PACS number(s): 76.70.Hb, 78.55.Kz, 73.61.Ph, 71.35.Aa

I. INTRODUCTION

Studies of optically detected magnetic resonances (ODMR) offer a unique probe of spin-dependent phenomena in organic semiconductors.[1] The technique is particularly useful for studying dark excitations—species that are normally incapable of photoluminescence, such as spin-1/2 polarons and spin-1 triplet excitons, large populations of which may be generated under sustained illumination. Recent interpretations of spin-1/2 ODMR experiments have been used to predict the relative formation rates of singlet (SE) and triplet (TE) excitons under electrical excitation,[2,3] a subject of great significance for optoelectronic applications of organic semiconductors. These and other interpretations of ODMR data, however, rely on a physical model of the origins of the spin-1/2 resonance that continues to be debated.[4] In this paper, we propose that interactions between TEs and polarons underlie the spin-1/2 ODMR, and that two types of polarons are present: short-lived paired polarons that may recombine after spin-dependent collisions with TEs, and long-lived unpaired polarons that are re-trapped before they can recombine. As a result, paired polarons are affected by magnetic resonance, and unpaired polarons are not. We are able to construct a full quantitative model of the ODMR on this basis that successfully models the measured frequency responses of resonant and photoinduced absorption data of the archetypal π-conjugated polymer poly[2-methoxy-5-(2-ethylhexyloxy)-1,4-phenylenevinylene] (MEH-PPV).

Resonance in the magnetic sublevel populations of polarons and TEs is induced when the frequency of an applied microwave field is tuned to the Zeeman splitting energy associated with an applied magnetic field. ODMR experiments measure spectroscopic changes caused by that resonance, for example, changes in photoinduced absorption detected magnetic resonances (PADMR) or in photoluminescence detected magnetic resonance (PLDMR). Although TE resonances are also commonly observed, the sharp, PL enhancing and PA quenching, spin-1/2 polaron resonance with g-factor $g=2.0025\pm0.0006$ (Refs. 1 and 5) has been studied most intensively and is the focus of this work. The increase in fluorescence ($\Delta PL>0$) and the decrease in polaron and TE densities ($\Delta PA<0$) under spin-1/2 resonance conditions have been well established in numerous prototypical polymers.[1,2,6–11]

Two types of models for the resonance have been proposed, based on recombination and quenching, respectively. Recombination models consider $\Delta PL>0$ to be a form of delayed fluorescence resulting from the recombination of slow (long-lived) polarons, and have been used to argue that SE formation is favored over TE formation in organic light emitting devices (OLEDs).[2,3] The recent observation of $\Delta PL>0$ under optical modulation frequencies orders of magnitude greater than the inverse polaron lifetime is, however, inconsistent with recombination.[4] Qualitatively, it is instead possible to explain the resonance with quenching models, under which $\Delta PL>0$ is due to reduced SE annihilation under resonance conditions. The SE population readily follows fast modulation since the singlet exciton lifetime is on the order of 1 ns. But the identity of the quenchers and the reason for their population change under resonance remain open questions. In this paper, we address these questions and build a quenching model of PLDMR experiments on MEH-PPV at low temperature. TE and polaron populations in MEH-PPV at 80 K are known experimentally to decrease under resonance.[12] Here we take into account SE quenching by both TE and polarons. In view of the limited charge mo-

bility at low temperature, we also distinguish between polarons trapped in pairs and isolated trapped polarons. We further identify the origin of the reduction of TE and polaron populations under resonance as TE-polaron quenching (TPQ). Spin-dependent processes involving TEs and electrons or holes are well known in organic molecular crystals.[13] The greater rate of TPQ under resonance is the basis for decreased quenching of SEs and is also consistent with $\Delta PA < 0$.

We focus in this paper on using the TPQ model to explain the dynamics of multiple quenching species, X, as measured by three experimental probes: (i) PLDMR, (ii) photoinduced absorption (PA), and (iii) double modulated PLDMR (DM-PLDMR). To briefly summarize the detailed analysis that follows this introduction, we note that in a quenching model, each SE quencher satisfies the steady-state relation

$$\frac{dS}{dt} = G_S - \frac{S}{\tau_S} - \gamma_{SX} X S = 0, \tag{1}$$

where G_S is the rate of generating SEs, S is the SE density, $\tau_S \approx 1$ ns, and γ_{SX} is the SE quenching rate. Since $\Delta PL > 0$ is a small ($<0.1\%$) correction to $S = G_S \tau_S$, the magnitude of the PLDMR under a quenching model is approximately

$$\Delta PL = S^* - S = S \tau_S \gamma_{SX} (X - X^*), \tag{2}$$

where the star indicates resonance conditions. The lifetime of SEs is much shorter than that of the long-lived quenching species. Thus, the frequency response of the PLDMR signal ΔPL provides a direct measurement of the dynamics of the quenching species, X, under microwave modulation. Alternately, we may measure the frequency response of X under optical modulation using PA. For the discussion that follows we define F_{XL} and F_{XM} as the frequency responses of X to light and microwave modulation respectively, normalized to unity at zero frequency.

Further insight is gained by studying polaron and exciton dynamics in a double modulated PLDMR (DM-PLDMR) experiment,[4] in which both the microwave field and the optical pump are modulated. Under a quenching model, DM-PLDMR has

$$X(t) = \overline{X}[1 + \alpha_L F_{XL}(\omega_L)\cos(\omega_L t)] \times [1 + \alpha_{XM} F_{XM}(\omega_M)\cos(\omega_M t)], \tag{3}$$

$$S(t) = \overline{S}[1 + \alpha_L \cos(\omega_L t)], \tag{4}$$

where bars indicate average values, α indicates modulation depth, and the zero-frequency light modulation depth is assumed to be the same for S and X. Detecting only that component that is modulated by both the optical pump and the microwave field, the DM-PLDMR signal under a quenching model is

$$\Delta PL|_{f_M, f_L} = \gamma_{SX} \alpha_L \alpha_M \overline{XS} F_{XM}(1 + F_{XL}). \tag{5}$$

Significantly, the DM-PLDMR frequency response of MEH-PPV has been observed[4] to be independent of the optical modulation frequency f_L for 1 kHz $< f_L <$ 100 kHz, invalidating spin-dependent recombination models of PLDMR. Equation (5) demonstrates that a quenching model successfully explains this flat response if F_{XL} is much less than unity over this frequency range, since F_{XL} is the only variable in Eq. (5) that depends on f_L. Direct measurements of F_{XL} show that this condition is satisfied,[4] and also that F_{XL} differs substantially from F_{XM}. In this work, we build a complete model of F_{XL} and F_{XM}, calculate the contributions to these responses of the various excited states in MEH-PPV, and demonstrate that F_{XL} and F_{XM} differ both because of the existence of distinct populations of paired and unpaired polarons, and also because of interactions among quenchers. This analysis considers a coupled system of three quenching species: TEs, paired polarons, and unpaired polarons—the populations of which all turn out to be interdependent and much larger than the SE population.

We construct a complete quantitative model of PLDMR below, and demonstrate that PLDMR frequency response data can be used to predict the dynamics of TEs, as well as that of paired and unpaired polarons. In Sec. II we describe theoretically the frequency dependencies expected under the TPQ model. In Sec. III, we review the experimental frequency dependence of MEH-PPV,[4] and in Sec. IV we compare it to the responses expected from the TPQ model. We show that this model can account for the measured data, and extract parameter values from a quenching fit to the data. We discuss the results in Sec. V, and in the conclusion, Sec. VI, we summarize the physics of the resonance and the properties of the various excited states of MEH-PPV. The linearized parameters used in the TPQ model are derived in Appendix A, and the frequency response of the spin-dependent recombination model is presented for completeness in Appendix B.

II. TE-POLARON QUENCHING MODEL

The generation of polarons and TEs is mediated by SEs, which are the primary excitations produced by an optical pump. Although only geminate pairs of polarons are formed by the dissociation of SEs, polaron spins are dephased and uncorrelated within 10–100 ns by hyperfine fields.[13] At low temperatures, polarons are localized by the disordered energetic environment of the amorphous polymeric film. Thus, even if the separation distance between oppositely charged polarons is short, the lifetime of the pair can exceed 100 μs. We distinguish here between polarons which are localized near an oppositely charged neighbor (paired polarons), and polarons which are not (unpaired polarons). Evidence for the existence of paired and unpaired polarons has been found in studies of the intensity dependence of the resonance[14] and in resonance line shapes.[15]

TEs are generated either from SEs by intersystem crossing or by the recombination of spin-randomized polarons. Since the radiative decay of TEs is retarded by spin conservation, TEs, like localized polarons, have long lifetimes. Indeed, the populations of polarons and TEs can easily exceed that of SEs under continuous illumination due to their long lifetimes, even though mostly SEs are generated directly by the optical pump.

Quenching of SEs by polarons and TEs has been invoked in several studies,[1,14–20] and the involvement of quenching

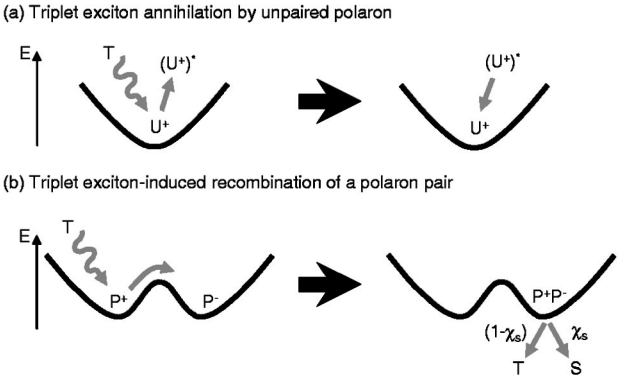

FIG. 1. Models for collision between a triplet exciton (TE) and (a) unpaired and (b) paired polarons at low temperature. In (a), a TE is annihilated by a solitary polaron. The polaron is excited by the collision but relaxes before it encounters an oppositely charged polaron, and is therefore unaffected by TE-polaron collisions or magnetic resonance. In (b), a pair of oppositely charged polarons are trapped in nearby energy wells. After collision with a TE, the TE is annihilated, and one of the polarons is excited, increasing its probability of crossing the energy barrier separating it from its oppositely charged partner. Assuming that the polarons are spin randomized, recombination creates a singlet exciton (SE) or a TE in the ratio $\chi_S:(1-\chi_S)$, otherwise only SEs are generated by polaron recombination.

processes has been suggested previously in interpretations of ODMR experiments.[1,14–16,19,20] But quenching interactions between SEs, and polarons or TEs, are not spin dependent and will therefore not be affected by resonance. Thus, quenching-dependent resonances must be due to spin-dependent interactions among the quenching species themselves. We propose here that the positive spin-1/2 and the spin-1 TE ODMR originate in the spin dependence of TE-polaron collisions. TE collisions with an unpaired and a paired polaron are shown schematically in Figs. 1(a) and 1(b), respectively. In both cases a TE gives up its energy to a polaron and the TE is quenched. The polaron is excited and is more likely to recombine if there is a nearby oppositely charged polaron. Thus, the collision leads to a decrease in the densities of TEs and *paired* polarons. The unpaired polaron density is unaffected: the excited polaron simply relaxes to its electronic ground state. In organic crystals[13] and OLEDs,[21] injected electrons or holes annihilate TEs by this mechanism.

The spin dependence of TE-polaron annihilation is a result of spin conservation. The system comprised of the colliding spin-1 TE and spin-1/2 polaron has six spin states of equal probability, two of which have spin 1/2. After the TE is quenched, a single excited polaron with spin-1/2 remains. Spin conservation therefore disallows 2/3 of TE-polaron collisions. Spin-1/2 resonance conditions induce rapid transitions between the spin-1/2 sublevels, so that all collisions become allowed. This increases the TE-polaron annihilation rate, drives down the paired polaron and TE densities, and reduces the rate of singlet quenching by those species.[13] Similarly, spin-1 resonance conditions also increase the TE-polaron annihilation rate and will reduce the rate of singlet quenching.

We now proceed to consider the dependence of the single-modulation PLDMR signal $\Delta\mathrm{PL}|_{\omega_M}$ on the microwave modulation frequency ω_M under the TPQ model. We assume throughout this paper that all polaron decay events produce singlet and TEs in the ratio $\chi_S:(1-\chi_S)$, where χ_S is some constant; see Fig. 1(b). The SE density S under the TPQ model is

$$\frac{dS}{dt} = -\frac{S}{\tau_S} - \gamma_{SP}S(P+U) - \gamma_{ST}ST + G_S + \chi_S\left(G_P - \frac{dP}{dt} + G_U - \frac{dU}{dt}\right), \tag{6}$$

where τ_S is the SE lifetime, P is the density of paired polarons, U is the density of unpaired polarons, T is the TE density, G_S is the singlet formation rate, G_P is the rate of generation of paired polarons, γ_{SP} is the interaction rate of SEs with paired and unpaired polarons, γ_{ST} is the interaction rate of SEs and TEs, and the recombination rates of paired and unpaired polarons are given generally by $G_P - dP/dt$ and $G_U - dU/dt$, respectively. Setting $dS/dt = 0$, Eq. (6) gives

$$S = G_S\tau_S[1 - \tau_S\gamma_{SP}(P+U) - \tau_S\gamma_{ST}T] + \chi_S\left(G_P - \frac{dP}{dt} + G_U - \frac{dU}{dt}\right)\tau_S, \tag{7}$$

where we have assumed that quenching will produce only a small perturbation on S, so that $\tau_S\gamma_{SP}(P+U) + \tau_S\gamma_{ST}T \ll 1$, and second-order delayed fluorescence has been ignored.

To determine the frequency dependence, we define $\mathbf{X}^{\ell,m}$ as the Fourier coefficient for a given modulated rate or species, $X(t)$, so that

$$X(t) = \mathrm{Re}\left\{\sum_{\ell,m}\mathbf{X}^{\ell,m}e^{i\ell\omega_L t + im\omega_M t}\right\}, \tag{8}$$

where a bold variable is complex and the superscripts ℓ and m refer to harmonics of ω_L and ω_M, respectively. Under the TPQ model, resonance leaves γ_{SP}, γ_{ST}, χ_S, and U unchanged but causes P and T to decrease through an enhanced TE-polaron interaction rate. Then from Eqs. (7) and (8), with $s = i\omega_M$,

$$\Delta\mathrm{PL}|_{\omega_M} = |\mathbf{S}^{0,1}| = G_S\tau_S\left| - \tau_S\gamma_{ST}\mathbf{T}^{0,1} - \mathbf{P}^{0,1}\left(\tau_S\gamma_{SP} + \frac{s}{G_S}\chi_S\right)\right|. \tag{9}$$

We can obtain the forms of $\mathbf{T}^{0,1}(\omega_M)$ and $\mathbf{P}^{0,1}(\omega_M)$ by considering the rate equations for TEs and polarons under the TPQ model

$$\frac{dP}{dt} = -\frac{P}{\tau_P} - \gamma_{TP}TP + G_P, \tag{10}$$

$$\frac{dT}{dt} = -\frac{T}{\tau_T} + (1-\chi_S)\left(\frac{P}{\tau_P} + \frac{U}{\tau_U}\right) - \chi_S\gamma_{TP}TP - \gamma_{TP}TU + G_T, \tag{11}$$

$$\frac{dU}{dt} = -\frac{U}{\tau_U} + G_U. \tag{12}$$

Here, γ_{TP} is the collision rate of TEs with both paired and unpaired polarons, where we assume that TEs will be annihilated and paired polarons will recombine with 100% probability; τ_P, τ_U, and τ_T are the paired polaron, unpaired polaron, and TE lifetimes respectively; and G_T is the rate of generation of TEs by intersystem crossing.

Since the changes in the polaron and TE populations under resonance are small, Eqs. (10)–(12) can be linearized to give the frequency response under microwave modulation predicted by the TPQ model. Since e^{st} (where s is complex) is an eigenfunction for all linear systems, the frequency responses of the linearized Eqs. (10)–(12) are the eigenvalues corresponding to the eigenfunction e^{st} with $s=i\omega_M$. We note that at high densities Eqs. (10)–(12) may not predict the correct steady-state values P_0, T_0, and U_0 due to the implicit linearization in the parameters τ_P, τ_T, and τ_U of any polaron-polaron or TE-TE bimolecular interactions. The equations are, however, valid for small-signal dynamics.

The TPQ model describes the quantities P, T, γ_{TP}, and γ_{TU} as changing under resonance. Taking γ_{TU} to be linearly proportional to γ_{TP}, P and T are linearized as

$$\frac{d}{dt}\begin{pmatrix} P-P_0 \\ T-T_0 \end{pmatrix} = \begin{pmatrix} P_P & P_T & P_\gamma \\ T_P & T_T & T_\gamma \end{pmatrix}\begin{pmatrix} P-P_0 \\ T-T_0 \\ \gamma_{TP}-\gamma_{TP0} \end{pmatrix}. \tag{13}$$

Here, a "0" subscript indicates a steady-state value, P_P is the derivative with respect to P of the right hand side of Eq. (10) at steady state, T_γ is the derivative with respect to γ_{TP} of the right hand side of Eq. (11) at steady state, and so on. The matrix elements in Eq. (13) are listed in Appendix A. Defining $P(t)-P_0=\mathrm{Re}\{\mathbf{P}^{0,1}e^{i\omega_M t}\}$ and similarly for $\mathbf{T}^{0,1}$, $\boldsymbol{\gamma}^{0,1}$, and then solving Eq. (13) with $s=i\omega_M$ gives

$$\frac{\mathbf{P}^{0,1}}{\boldsymbol{\gamma}^{0,1}} = \frac{sP_\gamma - T_T P_\gamma + T_\gamma P_T}{s^2 + s(-T_T - P_P) + (P_P T_T - T_P P_T)}, \tag{14}$$

$$\frac{\mathbf{T}^{0,1}}{\boldsymbol{\gamma}^{0,1}} = \frac{sT_\gamma - P_P T_\gamma + P_\gamma T_P}{s^2 + s(-T_T - P_P) + (P_P T_T - T_P P_T)}. \tag{15}$$

From Eqs. (9), (14), and (15), then, under the TPQ model, the single-modulation signal $\Delta\mathrm{PL}|_{\omega_M}$ will exhibit a two-pole frequency response.

We now consider the double-modulated signal $\Delta\mathrm{PL}|_{\omega_L,\omega_M}$. From Eq. (7), we obtain

$$\Delta\mathrm{PL}|_{\omega_L,\omega_M} = \mathrm{Re}\{\mathbf{S}^{1,1}\} = -\tau_S^2 \mathrm{Re}\left\{\begin{array}{c} \gamma_{ST}\mathbf{T}^{0,1}\mathbf{G}_\mathbf{S}^{0,0}\left(\dfrac{\mathbf{G}_\mathbf{S}^{1,0}}{\mathbf{G}_\mathbf{S}^{0,0}} + \dfrac{\mathbf{T}^{1,0}}{\mathbf{T}^{0,0}}\right) \\ + \gamma_{SP}\mathbf{P}^{0,1}\mathbf{G}_\mathbf{S}^{0,0}\left(\dfrac{\mathbf{G}_\mathbf{S}^{1,0}}{\mathbf{G}_\mathbf{S}^{0,0}} + \dfrac{\mathbf{P}^{1,0}}{\mathbf{P}^{0,0}}\right) \\ + \dfrac{\chi_S i(\omega_L+\omega_M)\mathbf{P}^{1,1}}{\tau_S} \end{array}\right\}. \tag{16}$$

The real part is taken because in the double lock-in experiment, the quenching contribution is small compared to the average PL, which is in phase with the optical modulation. An expression for $\mathbf{P}^{1,1}$ can be obtained by expanding Eqs. (10) and (11) in Fourier series, and substituting Eqs. (14), (15), (18), and (19). $\mathbf{P}^{1,1}$ falls to zero at high frequency. We obtain $\mathbf{P}^{1,0}(\omega_L)$ and $\mathbf{T}^{1,0}(\omega_L)$, and hence $\Delta\mathrm{PL}|_{\omega_L,\omega_M}$, by repeating the linearization of Eqs. (10) and (11) in the case that only the optical power is modulated. In that case, only the quantities P, T, U, G_P, G_T, and G_U vary, so that

$$\frac{d}{dt}\begin{pmatrix} P-P_0 \\ U-U_0 \\ T-T_0 \end{pmatrix} = \begin{pmatrix} P_P & 0 & P_T \\ 0 & U_U & 0 \\ T_P & T_U & T_T \end{pmatrix}\begin{pmatrix} P-P_0 \\ U-U_0 \\ T-T_0 \end{pmatrix} + \begin{pmatrix} G_P-G_{P0} \\ G_U-G_{U0} \\ G_T-G_{T0} \end{pmatrix}. \tag{17}$$

Here, U_U is the derivative with respect to U of the right hand side of Eq. (12), and so on. Analogous to the microwave-modulation case, we define $P(t)-P_0=\mathrm{Re}\{\mathbf{P}^{1,0}e^{i\omega_L t}\}$, and similarly for $\mathbf{U}^{1,0}$, $\mathbf{T}^{1,0}$, $\mathbf{G}_\mathbf{P}^{1,0}$, $\mathbf{G}_\mathbf{U}^{1,0}$, $\mathbf{G}_\mathbf{T}^{1,0}$. The matrix elements in Eq. (17) are listed in Appendix A, and its solution with $s=i\omega_L$ is

$$\frac{\mathbf{P}^{1,0}}{\mathbf{G}_\mathbf{P}^{1,0}} = \frac{s^2 + s\left[P_T\dfrac{G_T}{G_P} - (T_T+U_U)\right] - \dfrac{G_T}{G_P}U_U P_T + \dfrac{G_U}{G_P}T_U P_T + T_T U_U}{(s-U_U)[s^2 + s(-T_T-P_P) + (P_P T_T - T_P P_T)]}, \tag{18}$$

$$\frac{\mathbf{T}^{1,0}}{\mathbf{G}_\mathbf{P}^{1,0}} = \frac{s^2\dfrac{G_T}{G_P} + s\left[T_U\dfrac{G_U}{G_P} + T_P - \dfrac{G_T}{G_P}(U_U+P_P)\right] + \dfrac{G_T}{G_P}U_U P_P - \dfrac{G_U}{G_P}T_U P_P - T_P U_U}{(s-U_U)[s^2 + s(-T_T-P_P) + (P_P T_T - T_P P_T)]}. \tag{19}$$

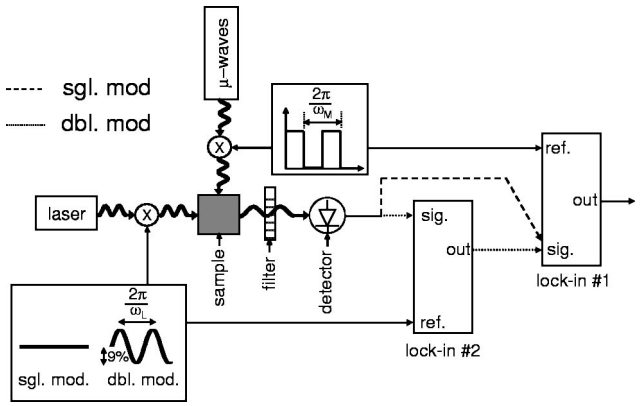

FIG. 2. The experimental setup for measuring the frequency response of the photoluminescence-detected magnetic resonance. The single-modulation result $\Delta PL|_{\omega_M}$ is measured with a single lock-in amplifier and microwave power modulation only, using the dashed signal path. The double-modulation result $\Delta PL|_{\omega_L,\omega_M}$ is measured with two lock-in amplifiers and both laser power and microwave power modulation, using the dotted signal path. Reproduced from Ref. 4.

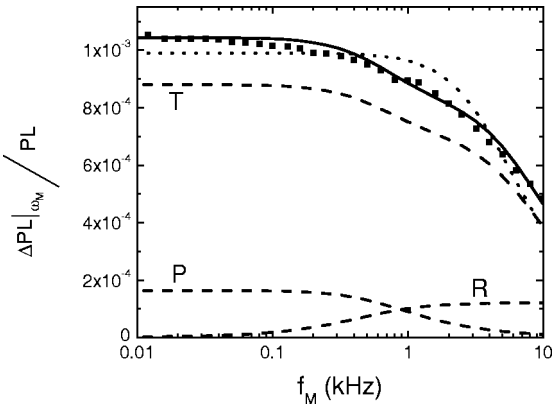

FIG. 3. Single modulation data $\Delta PL|_{\omega_M}/PL$ for MEH-PPV as a function of microwave modulation frequency $f_M=\omega_M/2\pi$. PL is average photoluminescence. The unlabeled solid line is the TPQ model fit to the data, given by Eqs. (9), (14), and (15), with triplet exciton (TE), paired and unpaired polaron lifetimes of 25 ± 3 μs, 325 ± 40 μs, and 8.6 ± 1.8 ms, respectively. The dashed lines break out contributions to the fit: T, P, and R are the contributions of TE quenching of singlet excitons (SEs), paired polaron quenching of SEs, and SE generation due to TE-induced recombination of paired polarons, respectively. The dotted line shows a single-pole fit. Frequency response data from Ref. 4.

Comparing Eqs. (18) and (19) to Eqs. (14) and (15), we see that the three poles of $\mathbf{P}^{1,0}$ and $\mathbf{T}^{1,0}$ include the two poles of $\mathbf{P}^{0,1}$ and $\mathbf{T}^{0,1}$, along with a pole at $s=U_U$. The simple form of this extra pole results from the fact that U is affected by the optical pump modulation but not by resonance.

Equation (16) shows that under the TPQ model, the double-modulation signal includes a contribution from quenching of singlet excitons by the steady-state or *average* populations of the quenching species ($\mathbf{P}^{0,1}$ and $\mathbf{T}^{0,1}$). This is a unique feature of the TPQ model, and is not found, for example, in the equivalent expression under the recombination model (see Appendix B), since in that model an average polaron population cannot contribute to the double-modulated signal. We find below that $\Delta PL|_{\omega_L,\omega_M}$ in MEH-PPV is dominated by the interaction between light-modulated SEs and the steady-state TE population, i.e., $\Delta PL|_{\omega_L,\omega_M} \propto \mathbf{T}^{0,1}\mathbf{G}_S^{1,0}$, and is independent of the optical modulation frequency ω_L for this reason.

III. EXPERIMENTAL DESIGN AND RESULTS

Figure 2 shows the experimental setups, described in Ref. 4, for measuring the dependence of the single-modulated signal $\Delta PL|_{\omega_M}$ on the microwave angular frequency ω_M, and the dependence of the double-modulated signal $\Delta PL|_{\omega_L,\omega_M}$ on the optical angular frequency ω_L. The sample was prepared by evaporating MEH-PPV films from a 3:7 THF:toluene solvent onto the inner walls of a glass capillary that was then evacuated and sealed. The MEH-PPV was illuminated by the $\lambda=488$ nm line of an Ar^+ laser with an intensity of 500 mW/cm^2 and subjected to spin-1/2 resonance conditions at X band ($\approx$9.35 GHz) at $T=20$ K. In the first experiment, the microwave field was square-wave modulated at ω_M and the ω_M component of the PL from the sample was measured by a lock-in amplifier. In the second experiment, in addition to this microwave modulation, the Ar^+ laser was sinusoidally modulated with amplitude ±8.8%. Two lock-in amplifiers were used in series, the first referenced to the modulation frequency ω_L of the laser and the second to ω_M. The time constant of the first lock in was set to 1 ms, small enough to allow through the ω_M sidebands on the ω_L "carrier" signal, although some sideband attenuation is introduced, and is corrected for in the data presented here. The frequency ω_M was varied in the first experiment, but held constant at $\omega_M=2\pi\times200$ Hz in the second experiment.

Figures 3 and 4 show the data reported previously in Ref. 4 for the single-modulation and double-modulation experiments, respectively. In both experiments the resonance was centered at 3.3 kG with a full width at half maximum of 13 G, indicating the same resonance was observed. The single-modulation data for MEH-PPV in Fig. 3 is fit poorly by a single pole (dotted line, Fig. 3). Much better fits are obtained using two poles (not shown), corresponding to lifetimes of 24 ± 3 and 244 ± 66 μs, suggesting that at least two species participate in the resonance together with SEs. The presence of two lifetimes is consistent with Eqs. (9), (14), and (15). These lifetimes may be directly assigned to TEs and polarons if these species are independent, however, in a coupled system such as the TPQ model of Eqs. (14) and (15), extraction of the TE and polaron lifetimes requires knowledge of the strength of the coupling between T and P; see Sec. IV below.

The contrast between the band-limited frequency response of the single-modulation case and the frequency-independent double-modulation data in Fig. 4 is a clear demonstration that spin-dependent polaron recombination (SDR) cannot be the origin of the PLDMR.[4] The expected response under the SDR model is shown in Fig. 4, normalized to the first data point (see Appendix B) and using the lifetime of the single-quencher fit in Fig. 3.

Both TEs and polarons are expected to quench singlet excitons. Under the TPQ model, we tentatively identify the

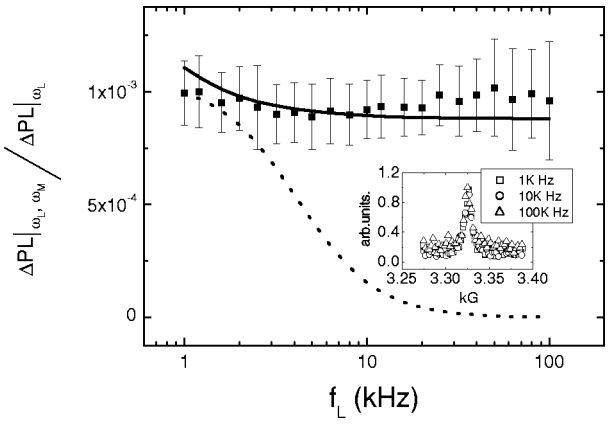

FIG. 4. Double modulation data $\Delta PL|_{\omega_L,\omega_M}/PL|_{\omega_L}$ for the same MEH-PPV sample as in Fig. 3 as a function of laser modulation frequency $f_L=\omega_L/2\pi$, with $f_M=\omega_M/2\pi$ held constant at 200 Hz. The solid and dotted lines are the predictions of the TPQ and SDR models, respectively. The SDR model prediction has been scaled to fit the data, and uses the single-lifetime fit of Fig. 3. The TPQ model prediction has been scaled down in magnitude by 16% to fit the data, and uses Eqs. (16), (18), and (19), with triplet exciton (TE), paired, and unpaired polaron lifetimes of 25 ± 3 μs, 325 ± 40 μs, and 8.6 ± 1.8 ms, respectively. Inset: $\Delta PL|_{\omega_L,\omega_M}/PL|_{\omega_L}$ line shapes as a function of magnetic field for $f_L=1$, 10, and 100 kHz are similar. Frequency response data from Ref. 4.

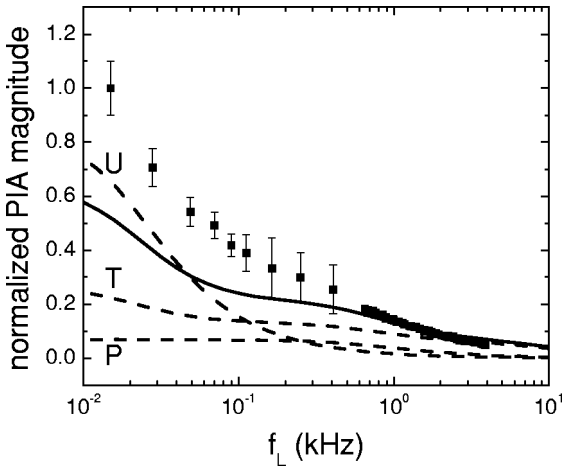

FIG. 5. Normalized photoinduced absorption (PA) magnitude measurement as predicted by the TPQ model (unlabeled solid line) and measured (points). The dashed lines break out contributions to the fit: T, P and U are the triplet exciton (TE), paired polaron, and unpaired polaron contributions, respectively. The T, P and U lifetimes as fit by the TPQ model are 25 ± 3 μs, 325 ± 40 μs, and 8.6 ± 1.8 ms, respectively. PA data from Ref. 4. The data has been normalized to the model prediction at $f_L=1660$ Hz. The small-signal approximation for the modulation of U breaks down at low frequencies.

dominant quencher in MEH-PPV to be TEs based on a measurement by Wei *et al.*[12] showing that the spectral overlap of the microwave-induced TE photoabsorption with the photoluminescent spectrum of MEH-PPV is much greater than the corresponding polaron overlap. Thus, from Eq. (16) the flat response in Fig. 4 in the frequency range $1\ \text{kHz} < f_L < 100$ kHz requires that over this range

$$\text{Re}\left\{\frac{\mathbf{T}^{1,0}}{\mathbf{T}^{0,0}}\right\} \ll \frac{\mathbf{G}_S^{1,0}}{\mathbf{G}_S^{0,0}}, \tag{20}$$

i.e., the in-phase optical modulation depth of the dominant quencher (TEs) at $f_L > 1$ kHz must be much less than the modulation depth of the optical pump (8.8%). The model parameters calculated in Sec. IV satisfy this condition.

Optical modulation of the quenching species in the absence of microwave modulation is examined in Fig. 5, which shows the results of a PA measurement of a drop-cast MEH-PPV film at $T=20$ K. The change in absorption by the sample of a probe laser on application of a $\lambda=405$ nm pump laser was measured as a function of the pump chop frequency. The probe wavelength, $\lambda=808$ nm, was selected to be as close as practical to the PL spectrum of MEH-PPV, thereby detecting quenchers with the best overlap with SEs, while also minimizing cross talk from optically modulated MEH-PPV PL.[4] The pump and probe lasers had intensities of 5 and 150 mW/cm^2, respectively.

The PA data measure the summed frequency responses of the absorption of U, P, and T at $\lambda=808$ nm. A good fit to the frequency response of the PA requires two poles. Least square fits yield lifetimes of 325 ± 40 μs and 8.6 ± 1.8 ms, where the error bars indicate a least squares error 10% greater than optimum. Comparing Eqs. (14) and (15) to Eqs. (18) and (19), the PA and single-modulation microwave response are expected to share two poles in common. This is indeed observed in the data: the pole corresponding to the 325 ± 40 μs lifetime measured from the PA data is consistent with the 244 ± 66 μs lifetime extracted from the microwave data. The highest frequency pole corresponding to the 24 ± 3 μs lifetime in the single-modulated microwave resonance data is also expected to be present in the PA data [see Eqs. (18) and (19)], but the PA data lack sufficient signal to noise to resolve this high frequency pole. In contrast, the low frequency pole corresponding to the 8.6 ± 1.8 ms lifetime is definitively not observed in the single-modulated microwave resonance data of Fig. 3. Under the TPQ model, the long 8.6 ± 1.8 ms lifetime results from the interaction of TE and SEs with unpaired polarons, the population of which is not affected by magnetic resonance. Figures 3 and 5 thus confirm the appearance of the three distinct species P, T, and U described in Sec. II above. These species are quantitatively analyzed in Sec. V below. Note that PA results consistent with those shown in Fig. 5 were also obtained by Smilowitz and Heeger, who measured the same absorption trend as in Fig. 5 at low frequencies in neat films of MEH-PPV, but measured a one-pole PA response when unpaired polaron formation was frustrated in a low density mixture of MEH-PPV in a polyethylene matrix.[22]

Slow dynamics of unpaired polarons within MEH-PPV are further examined in Fig. 6, which shows the slow transient PL response of a drop-cast MEH-PPV film at $T=20$ K in response to laser excitation at $\lambda=408$ nm. The steady-state quenching magnitude of the transient data in Fig. 6 defines the steady-state population of unpaired polarons, U_0, i.e.

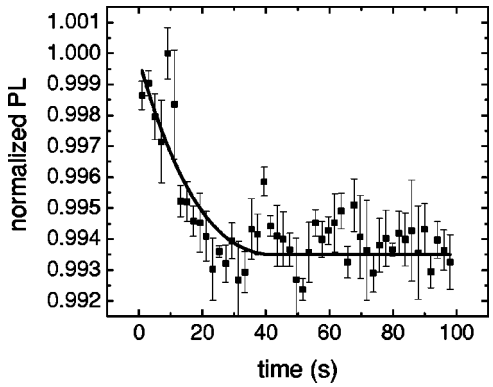

FIG. 6. Long-lived unpaired polarons are responsible for the slow transient response of the photoluminescence of a drop-cast MEH-PPV film at $T=20$ K. The solid line is a guide to the eye.

$$U_0 = 0.6\,\%/(\gamma_{SP}\tau_S). \tag{21}$$

The transient lifetime in Fig. 6 ($\approx$11 s) is three orders of magnitude longer than the linearized steady-state small signal lifetime 8.6 ± 1.8 ms, extracted from the low frequency pole in the PA data. This discrepancy is likely due to the presence of fast bimolecular decay processes in steady state.

Finally, Fig. 7 shows the double-modulation resonance line shape detected at the second light harmonic at $f_L = 10$ kHz, i.e., $\Delta\text{PL}|_{2\omega_L,\omega_M}$ normalized to $\Delta\text{PL}|_{2\omega_L}$. A second harmonic signal is expected if bimolecular processes are involved in the resonance, as is the case for both SDR and TPQ models. Under the TPQ model, if polaron quenching of SEs and SE generation by TE-induced recombination of polaron pairs are small relative to singlet-TE interactions, then $\Delta\text{PL}|_{2\omega_L,\omega_M}/\Delta\text{PL}|_{2\omega_L}$ gives the modulation depth of the TE population under microwave drive.

IV. ANALYSIS

We now evaluate the parameters in the TPQ model for consistent fits to the data in Figs. 3–6. Beginning with the PA

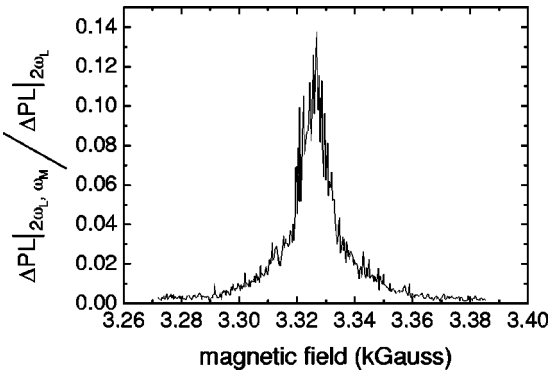

FIG. 7. Double-modulated resonance line shape detected at the second light harmonic frequency with $f_L=\omega_L/2\pi\doteq10$ kHz. A second harmonic signal is expected under the TPQ model. If polaron quenching of singlet excitons (SEs) and SE generation by triplet exciton (TE)-induced recombination of polaron pairs are small relative to SE-TE interactions, then $\Delta\text{PL}|_{2\omega_L,\omega_M}/\Delta\text{PL}|_{2\omega_L}$ gives the modulation depth of the TE population under microwave drive.

data, we require two poles, p_{A1} and p_{A2}, a zero z_A, and some scaling factor, c_A, for a good fit

$$\text{PA} = c_A\frac{(s+z_A)}{(s+p_{A1})(s+p_{A2})}. \tag{22}$$

A least squares fit returns the values $p_{A1}=3079$ rads/s, $p_{A2}=117$ rads/s, and $z_A=433$ rads/s. TEs and paired and unpaired polarons will contribute to the PA data so that PA $\propto\gamma_{ST}\boldsymbol{T}^{1,0}+\gamma_{SP}(\boldsymbol{U}^{1,0}+\boldsymbol{P}^{1,0})$, where the triplet absorption of the pump probe relative to the polaron absorption has been taken to be γ_{ST}/γ_{SP}. This expression is used to calculate the predicted PA in Fig. 5. For the purposes of obtaining fit parameters, however, we assume that the TEs dominate the PA. This is a reasonable assumption since overlap between TEs and the edge of the MEH-PPV PL spectrum at $\lambda=808$ nm is greater than the corresponding overlap with polarons.[12] In addition, the slow response of U minimizes its contribution at high frequencies. We find the assumption that the PA is proportional to $\boldsymbol{T}^{1,0}$ produces fit parameters that change little when $\boldsymbol{U}^{1,0}$ and $\boldsymbol{P}^{1,0}$ are also considered. We also note that the three poles of the PA frequency response are not changed by the relative absorption strengths of T, P, and U under the TPQ model.

The PA measurement is performed at low frequencies ($f_L<4$ kHz). Because we expect the TE lifetime $\tau_T<100$ μs, and we see only two poles in the PA, we set $dT/dt\approx0$ for the purposes of determining fit parameters from the PA data. Then Eqs. (10)–(12) can be solved to give a two-pole expression for $T^{1,0}$

$$T^{1,0}\approx\frac{-T_UG_U(s+1/\tau_P)-T_PG_P(s+1/\tau_U)}{T_T(s+1/\tau_U)(s+1/\tau_P)}, \tag{23}$$

where it has been assumed that TE-polaron quenching is negligible compared to the TE and polaron decay rates $1/\tau_T, 1/\tau_P$, respectively. Then, by comparing Eqs. (22) and (23), we identify

$$\tau_P = 1/p_{A1}, \tag{24}$$

$$\tau_U = 1/p_{A2}. \tag{25}$$

The single-modulation data $\Delta\text{PL}|_{\omega_M}/\text{PL}$ of Fig. 3 requires two poles, p_{M1} and p_{M2}, a zero, z_M, and some scaling factor, c_M for a good fit

$$\Delta\text{PL}|_{\omega_M}/\text{PL} = c_M\frac{(s+z_M)}{(s+p_{M1})(s+p_{M2})}. \tag{26}$$

A least squares fit returns the values $p_{M1}=4101$ rads/s, $p_{M2}=41393$ rads/s, and $z_M=5148$ rads/s. While under the TPQ model, p_{M1} and p_{A1} are the same pole (see Sec. II) and are measured to be within error of each other (see Sec. III), superior fits are obtained using their distinct fit values.

Assuming that TEs dominate the quenching and by comparing Eqs. (15) and (26), we obtain a set of simultaneous equations that can be solved for P_0, T_0, and τ_T

$$T_T + P_P = p_{M1} + p_{M2}, \tag{27}$$

$$P_P T_T - T_P P_T = p_{M1} p_{M2}, \tag{28}$$

$$\frac{P_P T_\gamma - P_\gamma T_P}{T_\gamma} = z_M. \tag{29}$$

The left hand sides of Eqs. (27)–(29) are related to P_0, T_0, and τ_T in Appendix A. Finally, by equating the zeros of Eqs. (22) and (23), we can solve for G_U

$$G_U = \frac{G_P T_P \tau_P (1 - \tau_U z_A)}{T_U \tau_U (\tau_P z_A - 1)}. \tag{30}$$

The parameters τ_P, τ_U, τ_T, P_0, T_0, and G_U are therefore set directly by the four poles and two zeros of the single-modulation and PA data. The singlet generation rate is calculated to be $G_S = 6 \times 10^{22}$ cm^{-3}/s based on an absorption length in MEH-PPV of 20 μm (Refs. 23 and 24) and an optical intensity of 500 mW/cm^2 measured at the sample. In fitting the data here, we use literature values for the following parameters: $\chi_S = 0.25$,[25] $\gamma_{ST} \approx 1 \times 10^{-9}$ cm^{-3}/s (Ref. 16) at $T = 10$ K, $\tau_S = 500$ ps,[26] and the intersystem crossing $G_T/G_S = 1\%$.[27] This leaves three free parameters to match the shape of the measured frequency responses: γ_{SP}, γ_{TP}, and G_P. Fitting yielded a polaron generation rate $G_P/G_S = 2.3\%$, a singlet-polaron quenching rate $\gamma_{SP} = \gamma_{ST}/22$, and a TE-polaron annihilation rate $\gamma_{TP} = 3 \times 10^{-15}$ cm^{-3}/s. The low γ_{SP} value is consistent with the relatively small spectral overlap of polarons with the PL spectrum of MEH-PPV.[12] The fitted γ_{TP} value is smaller than the TE-polaron interaction rate measured by Greenham *et al.*, which was 3×10^{-14} cm^{-3}/s at $T = 10$ K in poly(2-methoxy-5-(3′,7′-dimethyl)-octyloxy-*p*-phenylenevinylene) (OC1C10-PPV).[28] The TE-polaron interaction rate is expected to be material dependent; the presence of defect or traps reduces TE and polaron diffusion rates, lowering γ_{TP}. The change in γ_{TP} under resonance, $\gamma^{0,1}$, required to match the magnitude of $\Delta PL|_{\omega_M}/PL$ was found to be 19%.

From Eqs. (24) and (25), we calculate $\tau_P = 325 \pm 40$ μs and $\tau_U = 8.6 \pm 1.8$ ms, where the error bars indicate a least squares error 10% greater than optimum. From Eq. (21), we calculate $U_0 = (2.6 \pm 0.2) \times 10^{17}$ cm^{-3}. From Eqs. (27)–(29), we calculate $\tau_T = 25 \pm 3$ μs and find $T_0 = 3.3 \times 10^{17}$ cm^{-3} and $P_0 = 1.6 \times 10^{17}$ cm^{-3}. Finally, from Eq. (30), we find $G_U/G_S = 0.8\%$. The resulting fits using Eqs. (9), (14)–(16), (18), and (19) are shown as solid lines in Figs. 3–5, and are in good agreement with the data. We note that large changes in the unpaired polaron population U occur under low frequency optical modulation, and the small-signal approximation used in the analysis in Sec. II breaks down.

The reason for the flat DM-PLDMR signal can now be understood using the TPQ theory. In the fit presented above, triplets are the dominant quencher in MEH-PPV due to their large population (twice the population of paired polarons), and their strong overlap with SE emission, both as indicated by the fit value of singlet-triplet interactions ($\gamma_{ST}/\gamma_{SP} = 22$) and by literature.[12] Triplets are, however, very weakly modulated by changes in light power: with the model parameters listed above, an 8.8% modulation in the light power produces only a 1.6% modulation in the triplet population at low modulation frequency. This weak modulation results from the fact that increased light power also produces more polarons, which quench triplets. The weak response of the triplets to light modulation ensures that the dominant quenching interaction under double-modulation conditions is the annihilation of light-modulated SEs by the steady-state population of TEs, which is independent of ω_L. The requirement for a flat DM-PLDMR, Eq. (20), is satisfied. The resulting predicted $\Delta PL|_{\omega_L,\omega_M}/\Delta PL|_{\omega_L}$ magnitude under the TPQ model matches the measured data to within 16% across the entire measured frequency range.

V. DISCUSSION

As noted in Ref. 4, the observation of almost constant $\Delta PL > 0$ in the double-modulation experiments (Fig. 4) up to $f_L = 100$ kHz rules out spin-dependent recombination models, since the lifetimes of both polarons and TEs are too long to follow the optical modulation. In quenching models, by contrast, ΔPL depends on SEs. Our quantitative application of the TPQ model is, however, limited by familiar difficulties such as the wealth of possible bimolecular excitonic processes and the limited knowledge of rate parameters. We have taken rates from previous work whenever possible, and since charges are probably trapped at $T = 20$ K, we have neglected P-U interactions, leaving three free parameters to match the shape of the measured responses (γ_{ST}, γ_{TP}, and G_P) and a single parameter ($\gamma^{0,1}$) to scale the predicted $\Delta PL|_{\omega_M}/PL$ magnitude. Below, we first summarize other observations that are consistent with the TPQ model. We then comment on the novel aspects of TE-paired-polaron collisions in Fig. 1 and on the important parameter χ_S for the fraction of polarons that recombine as singlets.

In further support of the TPQ model, we note that: (i) Resonances originating in TE-polaron collisions have been previously observed in fullerenes.[29–31] (ii) The TPQ model is consistent with the trends in the densities of SEs, TEs, and polarons observed in PADMR.[2,3,6,7,32] (iii) The TPQ model is consistent with electroluminescence detected magnetic resonance signals that are anomalously small under the spin-dependent polaron recombination model.[25,33–36] (iv) Since TE-polaron interactions are independent of molecular weight, the TPQ model is also consistent with the PL- and electroluminescence-enhancing resonances in small molecular weight materials such as tris(8-hydroxyquinoline) aluminum (Alq_3).[34] (v) The TPQ model is consistent with a measured singlet ratio of $(20 \pm 4)\%$ in MEH-PPV.[25] (vi) Because a spin-1 resonance mixes TE spin sublevels, it will also increase the rate of TE-polaron collisions. The observation of both spin-1/2 and spin-1 resonances in ODMR is therefore consistent with the TPQ model. (vii) Other published measurements of the frequency response of the spin-1/2 PLDMR also exhibit a two-lifetime behavior consistent with the TPQ model [see Eqs. (9), (14), and (15)], including MEH-PPV,[8] 2,5-dioctoxy PPV,[9] PPV,[10] methyl-bridged ladder-type poly(*p*-phenylene),[15,2] and 2,5-dibutoxy poly (*p*-phenylene ethynylene).[11] Finally, (viii) the TPQ mechanism is, to our knowledge, the only mechanism that can account for the positive spin-1/2 electrically detected magnetic

resonance (EDMR) observed in current flow through polymeric and small-molecular OLEDs under bias.[34,35] We speculate that the increase in current under resonance is due to polarons that are excited or detrapped by interactions with TEs.

Although there are numerous precedents for spin-dependent TE-polaron annihilation, no special role has been proposed for the excited polaron that is generated. Rapid vibronic relaxation to the electronic ground state is expected. For a TE collision with a paired polaron at low T, as sketched in Fig. 1(b), excitation can also promote recombination. The contribution of this recombination process to $\Delta\mathrm{PL}|_{\omega_M}/\mathrm{PL}$ with the present parameters is labeled "R" in Fig. 3. This novel γ_{TP} process in Eq. (10) is an additional mechanism coupling the TE and polaron populations. The steady-state populations are thus strongly coupled in our analysis.

The steady-state values for P, T, and U listed in Sec. V above are calculated from Eqs. (24)–(29), rather than from the rate equations for those species, Eqs. (10)–(12), which may not produce accurate steady-state values because they do not include bimolecular interactions that are important at high densities. Solving for the steady-state values from the rate equations gives $P_0=4.4\times10^{17}$ cm^{-3}, $T_0=3.7\times10^{16}$ cm^{-3}, and $U_0=4.3\times10^{18}$ cm^{-3}, as compared to the linearized fit values $P_0=1.6\times10^{17}$ cm^{-3}, $T_0=3.3\times10^{17}$ cm^{-3}, and $U_0=(2.6\pm0.2)\times10^{17}$ cm^{-3}. In our experiments, we have $S=3\times10^{13}$ cm^{-3} and since SE-SE annihilation is less than 1% of G_S for a typical $\gamma_{SS}=10^{-8}$ cm^{-3}/s,[13] we have not included this term in Eq. (6).

We have used $\chi_S=0.25$, the statistical value for recombination of spin-1/2 polarons into SEs, but the present data do not constrain this interesting parameter directly. There is an indirect connection, however, since $\chi_S>0.25$ has been inferred from ΔPL measurements on conjugated polymers at low temperature, including MEH-PPV, that were analyzed in terms of faster polaron recombination under resonance conditions. Theoretical arguments for $\chi_S>0.25$ have been advanced for such recombination,[2,3,6] motivated by these data. Quenching models that include spin-dependent TE-polaron processes account for $\Delta\mathrm{PL}>0$ without so far having to invoke $\chi_S>0.25$.

VI. CONCLUSION

The TE-polaron quenching (TPQ) model ascribes the photoluminescence-detected magnetic resonance to a reduction in the singlet quenching rate caused by an increased rate of TE-polaron collisions under resonance. The TPQ model can fully account for the measured photoinduced absorption, single-modulation PLDMR, and double-modulation PLDMR frequency responses of the archetypal π-conjugated polymer MEH-PPV. With just four free parameters, the TPQ model successfully reproduces the shapes of these three independent frequency responses over decades of frequency, as well as the magnitudes of the two PLDMR frequency responses. A frequency analysis of the spin-dependent polaron recombination model confirms that it cannot account for these measurements.[4] The flat double-modulation PLDMR frequency response is explained by the TPQ model as resulting from singlet quenching by an average quencher population.

The existence of unpaired polarons is clearly indicated by a low frequency pole in the photoabsorption (PA) data, which is not present in the PLDMR frequency response. Using the TPQ model, we thus find three SE quenching species and their lifetimes: paired polarons with $\tau_P=325\pm40$ μs, unpaired polarons with $\tau_U=8.6\pm1.8$ ms, and TEs with $\tau_T=25\pm3$ μs. Paired polarons may recombine after being excited by collisions with TEs. Unpaired polarons are similarly excited by collisions with TE excitons, but are retrapped before they are able to recombine, and so are unaffected by resonance, although they may be the source of the positive spin-1/2 EDMR observed in polymeric and small-molecular weight OLEDs at low temperatures.[34,35] Photoinduced absorption measurements modulate all three quenchers, and therefore exhibit three lifetimes, while magnetic resonance measurements do not modulate unpaired polarons and therefore exhibit only two lifetimes. Parameter values such as lifetimes and populations can be extracted from these measured frequency responses using the TPQ model.

ACKNOWLEDGMENTS

The work at MIT was supported primarily by the MRSEC Program of the National Science Foundation under Award No. DMR 02-13282. Ames Laboratory is operated by Iowa State University for the U.S. Department of Energy under Contract No. W-7405-Eng-82. The work at the Ames Laboratory was supported by the Director for Energy Research, Office of Basic Energy Sciences, DOE.

APPENDIX A: LINEARIZED PARAMETERS IN TH TE-POLARON QUENCHING MODEL

The constants used in the linearized Eqs. (13) and (17) have the form X_Y and are the derivatives of X with respect to Y for Y at steady state. They are obtained from the expressions for P, T, and U in Eqs. (10)–(12)

$$P_P = -\frac{1}{\tau_P} - \gamma_{TP0}T_0, \tag{A1}$$

$$P_T = -\gamma_{TP0}P_0, \tag{A2}$$

$$P_\gamma = -T_0P_0, \tag{A3}$$

$$T_P = -\chi_S\gamma_{TP0}T_0 + (1-\chi_S)\frac{1}{\tau_P}, \tag{A4}$$

$$T_T = -\frac{1}{\tau_T} - \chi_S\gamma_{TP0}P_0 - \gamma_{TP0}U_0, \tag{A5}$$

$$T_U = \frac{(1-\chi_S)}{\tau_U} - \gamma_{TP0}T_0, \tag{A6}$$

$$T_\gamma = -\chi_S T_0P_0 - T_0U_0 \quad \text{and} \tag{A7}$$

$$U_U = -\frac{1}{\tau_U}. \tag{A8}$$

APPENDIX B: SPIN-DEPENDENT RECOMBINATION MODEL

We consider below the dependence under the spin-dependent recombination (SDR) model of the single-modulated PLDMR signal $\Delta\mathrm{PL}|_{\omega_M}$ on microwave modulation frequency ω_M, and the double-modulated signal $\Delta\mathrm{PL}|_{\omega_L,\omega_M}$ on optical modulation frequency ω_L.[2] Following Ref. 32, we consider only unpaired polarons U and treat unpaired polaron recombination as a bimolecular process, so that the SE density S is

$$\frac{dS}{dt} = -\frac{S}{\tau_S} + \chi_S \gamma_{UU} U^2 + G_S, \tag{B1}$$

where γ_{UU} is the interaction rate of unpaired polarons. When all modulation frequencies are much smaller than $1/\tau_S$, we may set $dS/dt=0$ so that Eq. (B1) gives

$$S = \chi_S \gamma_{UU} U^2 \tau_S + G_S \tau_S. \tag{B2}$$

Under the SDR model, resonance causes the SE fraction χ_S and the unpaired polaron recombination rate γ_{UU} to increase. Then from Eqs. (B2) and (8) the single-modulated PLDMR signal will be

$$\Delta\mathrm{PL}_{\omega_M} = |\mathbf{S}^{0,1}| = \tau_S \left| \boldsymbol{\chi}_{\mathbf{S}}^{0,1} \boldsymbol{\gamma}_{\mathbf{UU}}^{0,0} (\mathbf{U}^{0,0})^2 + \boldsymbol{\chi}_{\mathbf{S}}^{0,0} \boldsymbol{\gamma}_{\mathbf{UU}}^{0,1} (\mathbf{U}^{0,0})^2 + 2\boldsymbol{\chi}_{\mathbf{S}}^{0,0} \boldsymbol{\gamma}_{\mathbf{UU}}^{0,0} \mathbf{U}^{0,0} \mathbf{U}^{0,1} \right|. \tag{B3}$$

The quantities $\boldsymbol{\chi}_{\mathbf{S}}^{0,1}$ and $\boldsymbol{\gamma}_{\mathbf{UU}}^{0,1}$ are independent of the microwave modulation frequency and so the first and second terms of Eq. (B3) produce only a constant offset, and the dependence of $\Delta\mathrm{PL}|_{\omega_M}$ on ω_M comes entirely from the last term. We can obtain the form of $\mathbf{U}^{0,1}(\omega_M)$ by considering the rate equation for polarons under the SDR model[6]

$$\frac{dU}{dt} = -\gamma_{UU} U^2 + G_U, \tag{B4}$$

where G_U is the rate of generation of unpaired polarons. Since the variation in U will be small, Eq. (B4) can be linearized to give

$$\frac{\mathbf{U}^{0,1}}{\boldsymbol{\gamma}_{\mathbf{UU}}^{0,1}} = \frac{-(\mathbf{U}^{0,0})^2}{s + 2\boldsymbol{\gamma}_{\mathbf{UU}}^{0,0} \mathbf{U}^{0,0}}. \tag{B5}$$

Equation (B5) shows that under the SDR model, the frequency response of the single-modulated signal $\Delta\mathrm{PL}|_{\omega_M}$ is described by a single pole equal to $2\boldsymbol{\gamma}_{\mathbf{UU}}^{0,0}\mathbf{U}^{0,0}$.

We turn now to the double-modulated signal $\Delta\mathrm{PL}|_{\omega_L,\omega_M}$. By expanding Eq. (B2) in a Fourier series, it can be shown that $\Delta\mathrm{PL}|_{\omega_L,\omega_M} = |\mathbf{S}^{1,1}|$ falls at least as fast with ω_L as does $\mathbf{U}^{1,0}$. By linearizing Eq. (B4) under double modulation, we obtain

$$\frac{\mathbf{U}^{1,0}}{\mathbf{G}_{\mathbf{U}}{}^{1,0}} = \frac{1}{s + 2\boldsymbol{\gamma}_{\mathbf{UU}}^{0,0} \mathbf{U}^{0,0}}, \tag{B6}$$

where $s = i\omega_L$. Comparing Eq. (B6) to Eq. (B5) then shows that under the SDR model, the double-modulated signal $\Delta\mathrm{PL}|_{\omega_L,\omega_M}$ must fall at least as fast with ω_L as the single-modulated signal $\Delta\mathrm{PL}|_{\omega_M}$ does with ω_M. In contrast, the TPQ model predicts a double-modulated signal that is a constant independent of ω_L for high ω_L. The SDR model prediction shown in Fig. 4 is a conservative estimate, where $\Delta\mathrm{PL}|_{\omega_L,\omega_M}$ is described by the same single pole that describes $\Delta\mathrm{PL}|_{\omega_M}$.

*Corresponding authors. Email addresses: baldo@mit.edu, shinar@ameslab.gov

[1] J. Shinar, in *Handbook of Organic Conductive Molecules and Polymers*, edited by H. S. Nalwa (Wiley, New York, 1997), p. 319.
[2] M. Wohlgenannt, K. Tandon, S. Mazumdar, S. Ramasesha, and Z. V. Vardeny, Nature (London) **409**, 494 (2001).
[3] M. Wohlgenannt, X. M. Jiang, Z. V. Vardeny, and R. A. J. Janssen, Phys. Rev. Lett. **88**, 197401 (2002).
[4] M. K. Lee, M. Segal, Z. G. Soos, J. Shinar, and M. A. Baldo, Phys. Rev. Lett. **94**, 137403 (2005).
[5] V. Dyakonov, G. Zoriniants, M. Scharber, and C. J. Brabec, Phys. Rev. B **59**, 8019 (1999).
[6] M. Wohlgenannt, C. Yang, and Z. V. Vardeny, Phys. Rev. B **66**, 241201 (2002).
[7] M. Wohlgenannt, W. Graupner, G. Leising, and Z. V. Vardeny, Phys. Rev. B **60**, 5321 (1999).
[8] D. S. Ginger and N. C. Greenham, Phys. Rev. B **59**, 10622 (1999).
[9] X. Wei, B. C. Hess, Z. V. Vardeny, and F. Wudl, Phys. Rev. Lett. **68**, 666 (1992).
[10] N. F. Colaneri, D. D. C. Bradley, and R. H. Friend, Phys. Rev. B **42**, 11670 (1990).
[11] J. Partee, J. Shinar, G. Leising, S. W. Jessen, A. J. Epstein, Y. Ding, and T. J. Barton, Proc. SPIE **3145**, 118 (1997).
[12] X. Wei, Z. V. Vardeny, N. S. Sariciftci, and A. J. Heeger, Phys. Rev. B **53**, 2187 (1996).
[13] M. Pope and C. Swenberg, *Electronic Processes in Organic Crystals* (Oxford University Press, Oxford, 1982).
[14] E. J. W. List, C.-H. Kim, A. K. Naik, U. Scherf, G. Leising, W. Graupner, and J. Shinar, Phys. Rev. B **64**, 155204 (2001).
[15] W. Graupner, J. Partee, J. Shinar, G. Leising, and U. Scherf, Phys. Rev. Lett. **77**, 2033 (1996).
[16] E. J. W. List, U. Scherf, K. Mullen, W. Graupner, C.-H. Kim, and J. Shinar, Phys. Rev. B **66**, 235203 (2002).
[17] S. Hayashi, K. Kaneto, and K. Yoshino, Solid State Commun. **61**, 249 (1987).
[18] D. D. C. Bradley and R. H. Friend, J. Phys.: Condens. Matter **1**, 3671 (1989).
[19] Z. V. Vardeny and X. Wei, Mol. Cryst. Liq. Cryst. Sci. Technol., Sect. A **256**, 465 (1994).
[20] E. J. W. List, C.-H. Kim, W. Graupner, G. Leising, and J. Shinar,

Synth. Met. **119**, 511 (2001).
[21] M. A. Baldo and S. R. Forrest, Phys. Rev. B **64**, 085201 (2001).
[22] L. Smilowitz and A. Heeger, Synth. Met. **48**, 193 (1992).
[23] S.-H. Lim, T. G. Bjorklund, and C. J. Bardeen, J. Chem. Phys. **118**, 4297 (2003).
[24] S.-H. Jin, M.-S. Jang, and H.-S. Suh, Chem. Mater. **14**, 643 (2002).
[25] M. Segal, M. A. Baldo, R. J. Holmes, S. R. Forrest, and Z. G. Soos, Phys. Rev. B **68**, 075211 (2003).
[26] L. Smilowitz, A. Hays, A. J. Heeger, G. Wang, and J. E. Bowers, Synth. Met. **55**, 249 (1993).
[27] H. D. Burrows, J. S. de Melo, C. Serpa, and L. G. Arnaut, J. Chem. Phys. **115**, 9601 (2001).
[28] A. S. Dhoot, D. S. Ginger, D. Beljonne, Z. Shuai, and N. C. Greenham, Chem. Phys. Lett. **360**, 195 (2002).
[29] P. A. Lane, L. S. Swanson, Q.-X. Ni, J. Shinar, J. P. Engel, T. J. Barton, and L. Jones, Phys. Rev. Lett. **68**, 887 (1992).
[30] C. A. Steren, H. van Willigen, and M. Fanciulli, Chem. Phys. Lett. **245**, 244 (1995).
[31] P. A. Lane and J. Shinar, Phys. Rev. B **51**, 10028 (1995).
[32] M. Wohlgenannt and Z. V. Vardeny, Synth. Met. **125**, 55 (2002).
[33] L. S. Swanson, J. Shinar, A. R. Brown, D. D. C. Bradley, R. H. Friend, P. L. Burn, A. Kraft, and A. B. Holmes, Phys. Rev. B **46**, 15072 (1992).
[34] G. Li, C.-H. Kim, P. A. Lane, and J. Shinar, Phys. Rev. B **69**, 165311 (2004).
[35] N. C. Greenham, J. Shinar, J. Partee, P. A. Lane, O. Amir, F. Lu, and R. H. Friend, Phys. Rev. B **53**, 13528 (1996).
[36] M. Wohlgenannt, Phys. Status Solidi A **201**, 1188 (2004).